

Translational Initiation Factor IF2 from *Bacillus stearothermophilus*: a Spectroscopic and Microcalorimetric Study of the C-Domain[†]

Rolf Misselwitz,[‡] Karin Welfle,[§] Christoph Krafft,[‡] Claudio O. Gualerzi,^{||} and Heinz Welfle^{*,‡}

Institute of Biochemistry, Medical Faculty (Charité), and Institute of Biology, Math.-Nat. Faculty I, Humboldt University, c/o Max-Delbrück-Centre for Molecular Medicine, Berlin, Germany, and Laboratory of Genetics, Department of Biology, University of Camerino, Italy

Received October 17, 1996; Revised Manuscript Received January 7, 1997[⊗]

ABSTRACT: Conformation and stability of the C-terminal domain of initiation factor IF2 from *Bacillus stearothermophilus* were analyzed by circular dichroism, fluorescence and Raman spectroscopy, and microcalorimetry under different solvent conditions. From circular dichroism and Raman measurements, IF2C at neutral pH can be classified as an $\alpha + \beta$ protein. Solvent perturbation and Raman spectroscopy indicate a high accessibility of the tyrosine residues in the native protein. The Gdn/HCl-induced unfolding of IF2C was monitored by circular dichroism. IF2C unfolding at neutral pH proceeds in two discrete steps. The midpoints (c_m) and the free energy of unfolding ($\Delta G_u^{\text{H}_2\text{O}}$) of the first and second transition are 2.05 M and 6.2 kcal·mol⁻¹ and 4.1 M and 12.9 kcal·mol⁻¹, respectively. ANS does not bind to the stable intermediate formed at 3 M Gdn/HCl. It seems likely that IF2C is composed of two subdomains which unfold in a stepwise process. Melting experiments at pH 7.0 are impaired by irreversible aggregation at higher temperatures. However, in Gdn/HCl containing buffer at denaturant concentrations up to 1.5 M the melting becomes a reversible process and can be analyzed by differential scanning calorimetry. At Gdn/HCl concentrations between 1.0 and 1.5 M, IF2C seems to be composed of two folding units with T_m values of about 60 and 78 °C and folding enthalpy values (ΔH_m) of about 37 and 58 kcal·mol⁻¹. At pH values below pH 3.0, IF2C can adopt a new acid-induced conformation, which is characterized by a high secondary structure content and a strong ANS binding. The Gdn/HCl-induced unfolding of IF2C at pH 2.6 takes place only in one discrete step with a midpoint c_m of 3.3 M and a $\Delta G_{\text{AUa}}^{\text{H}_2\text{O}}$ of 11.9 kcal·mol⁻¹.

Translational initiation factor IF2¹ is involved in the initiation step of translation in prokaryotes and belongs to the family of GTP/GDP binding proteins. The genetic, functional, and structural aspects of these proteins were recently reviewed (Spurio et al., 1993). IF2 is involved in the interactions with at least four components of the initiation step, GTP, 30S and 50S ribosomal subunits, and fMet-tRNA^{fMet}, and may also play additional roles in other cellular processes, such as transcription (Travers et al., 1980) or protein secretion (Shiba et al., 1986).

The gene for the *Bacillus stearothermophilus* translational initiation factor IF2 was cloned, and it codes for a protein of 742 amino acids (Brombach et al., 1986). Sequence alignment with IF2 molecules of other organisms shows a

high homology in the C-terminal part comprising two-thirds of the sequence but only a little homology in the N-terminal region of the molecules (Brombach et al., 1986; Spurio et al., 1993). Limited proteolysis of IF2 in the presence and absence of GTP (Severini et al., 1990) and of fMet-tRNA^{fMet} (Severini et al., 1992) generates two trypsin resistant polypeptide chains corresponding to a central 40 kDa G-fragment and a 24.5 kDa C-terminal fragment, whereas the N-terminal part is very readily cleaved into small fragments indicating a loose and flexible structure. The two compact G- and C-fragments were obtained as recombinant proteins by genetic manipulation of the *B. stearothermophilus* *infB* gene and expression in *Escherichia coli* (Gualerzi et al., 1991; Spurio et al., 1993).

The C-terminal part of the translational initiation factor IF2 from *B. stearothermophilus* (IF2C) contains the fMet-tRNA^{fMet} binding site of IF2 (Gualerzi et al., 1991). IF2C represents a compact fold which is relatively resistant against further proteolytic degradation in the presence and absence of GTP (Severini et al., 1990; Gualerzi et al., 1991). A large deletion of 134 amino acids in the middle of IF2C is connected with the loss of the fMet-tRNA^{fMet} binding ability (Spurio et al., 1993).

Up to now, rather limited structural data for the intact IF2 molecule and the stable fragments IF2G and IF2C are available. The most relevant information on the 3D structure exists for the GTP/GDP-binding domain resulting from the comparison with other G-proteins of known tertiary structure, e.g., with the elongation factor EF-Tu (Cenatiempo et al.,

[†] C.O.G. was the recipient of an Alexander von Humboldt Forschungspreis.

* Address correspondence to this author at Max-Delbrück-Centre for Molecular Medicine, Robert-Rössle-Str. 10, D-13122 Berlin, Germany. Tel: +49 30 9406 2840. Fax: +49 30 9406 2840. E-mail: welfle@orion.rz.mdc-berlin.de.

[‡] Institute of Biochemistry.

[§] Institute of Biology.

^{||} University of Camerino.

[⊗] Abstract published in *Advance ACS Abstracts*, February 15, 1997.

¹ Abbreviations. IF2, translational initiation factor 2; IF2C, C-terminal domain of initiation factor 2 from *B. stearothermophilus*; I-form, intermediate state of IF2C; A-form, acid-induced state of IF2C; Gdn/HCl, guanidine hydrochloride; ANS, 8-anilino-1-naphthalenesulfonate; HEPES, 2-[4-(2-hydroxyethyl)-1-piperazinyl]ethanesulfonic acid; CD, circular dichroism; DSC, differential scanning calorimetry; $[\Theta]_{220}$, molar mean residue ellipticity at 220 nm; ΔG_{NI} , ΔG_{IU} , and ΔG_{AUa} , free energy of unfolding of native (N→I), intermediate (I→U), and acid-induced (A→U_a) states, respectively.

1987; Clark et al., 1990) and the H-ras p21 oncogen protein (Pai et al., 1990).

Here we present data on the conformation and stability of IF2C at neutral and acidic pH using various spectroscopic and microcalorimetric measurements. We have found that IF2C can adopt distinct conformational states depending on the environmental conditions. Unfolding under native conditions proceeds via a stable intermediate state in a well-separated two-step process. These results shall finally contribute to a complete understanding of the structure–function relationships of IF2 in the process of protein biosynthesis, especially in combination with the results of ongoing X-ray diffraction studies on complexes of IF2C with fMet-tRNA^{fMet} (U. Heinemann and C. O. Gualerzi et al., unpublished results).

MATERIALS AND METHODS

Chemicals. Ultrapure guanidine hydrochloride (Gdn/HCl) was from ICN Biomedicals (Cleveland, OH) and was used without further purification. Sodium cacodylate and 8-anilino-1-naphthalenesulfonate (ANS) were from Serva (Heidelberg, Germany). Dimethyl sulfoxide, HEPES, and Carbowax 300 were obtained from Merck (Darmstadt, Germany). *N*-Acetyl-L-tyrosine ethyl ester was from Schwarz/Mann (U.S.A.).

Cloning, Expression, and Purification. The *B. stearothermophilus* IF2C-domain was hyperproduced from the expression vector pXR401C constructed as previously described (Spurio, et al. 1993). The high-salt (1 M NH₄Cl) post-ribosomal supernatant was prepared essentially as described (Pawlik et al., 1981) and, after 40-fold dilution with buffer A [20 mM Tris-HCl, pH 7.1, 1 mM EDTA, 5 mM 2-mercaptoethanol, and 10% (v/v) glycerol], was loaded on a DEAE-cellulose column equilibrated with buffer A containing 25 mM NH₄Cl and eluted with a linear gradient (25–300 mM) in buffer A. The fractions containing the C-domain were pooled and concentrated by an Amicon ultrafiltration device. To remove the extra amino acids added to the N-terminus of the C-domain by cloning manipulations, the protein was subjected to proteolysis with trypsin (treated with L-1-tosylamido-2-phenylethyl chloromethyl ketone) for 1 h at 37 °C (Gualerzi et al., 1991). The reaction was stopped by addition of soybean trypsin inhibitor and the protein was purified on a DEAE-cellulose column under the same conditions described above.

Sample Preparation. Before spectroscopic and microcalorimetric measurements the IF2C samples were dialyzed exhaustively against 2 mM sodium cacodylate, pH 7.0, 0.5 M NaCl, 5 mM MgCl₂ and subjected to gel filtration on a Superose 12 column (Pharmacia, Uppsala, Sweden) equilibrated against the same buffer. The peak fractions were collected and dialyzed against appropriate buffers as indicated in the text. Protein samples at various pH values were prepared in 2 mM sodium cacodylate by titration with NaOH or HCl.

For Raman measurements the protein solution was concentrated in Microcon tubes (Amicon, Germany) with 10 kDa cutoff and transferred into 20 mM HEPES/KOH, pH 6.6, 5 mM MgCl₂ by Sephadex G-10 filtration.

Protein concentrations were determined spectrophotometrically at 276 nm using an absorption coefficient of 0.424 mL·mg⁻¹·cm⁻¹. The absorption coefficient was calculated from the amino acid composition, with seven tyrosine

residues, and a molar mass of 24452 g·mol⁻¹ as described previously (Mach et al. 1992).

FPLC Measurements. Analytical gel filtration was performed at 20 °C on a Pharmacia FPLC system. Protein samples of about 1 mg·mL⁻¹ in 2 mM sodium cacodylate buffer, pH 7.0, in the presence of various salts were applied to a calibrated Superose 12 HR 10/30 column equilibrated in the appropriate buffers.

Circular Dichroism. CD measurements were performed as described recently (Misselwitz et al., 1995) at 25 °C with a Jasco J-720 spectropolarimeter. The instrument was equipped with a thermostated cell holder and a temperature control system (Neslab, U.S.A.). Temperature scans were performed with a heating rate of 20 °C·h⁻¹. Mean residue ellipticities [Θ] were calculated using a mean residue mass of 110.1 Da. Far-ultraviolet CD spectra were measured with a cuvette of 0.010 cm path length and a protein concentration of 0.80 mg·mL⁻¹ or with a 0.10 cm cell and a protein concentration of 0.080 mg·mL⁻¹ in the case of denaturant-induced unfolding and refolding experiments. CD spectra in the near-ultraviolet region were registered in a 0.50 cm cell at a protein concentration of 3.9 mg·mL⁻¹.

The secondary structure content was calculated from the far-ultraviolet CD spectra using the variable selection method (program VARSLC1) starting with a set of 33 reference proteins (Johnson, 1990).

Fluorescence Measurements. Fluorescence spectra were measured at 25 °C with a Shimadzu fluorimeter RF-5001PC. Tyrosine fluorescence spectra and ANS fluorescence spectra were measured with excitation wavelengths of 276 and 365 nm, respectively. All measurements were performed with 5 nm bandwidths for both the excitation and emission monochromator. The absorbance of all samples was less than 0.1 absorbance units at the excitation wavelength. Fluorescence spectra were corrected for contributions of buffer and denaturing agent and normalized with respect to the protein concentration and the Raman band of water which was used as an internal intensity standard.

Solvent Perturbation Spectroscopy. Solvent perturbation measurements were performed as described earlier (Misselwitz et al., 1975). The perturbation spectra of IF2C and the model compound *N*-acetyl-L-tyrosine ethyl ester were recorded at 25 °C on a Kontron 930 spectrophotometer in tandem mix cells (Hellma, Müllheim, Germany) in the presence of 20% (v/v) dimethyl sulfoxide or polyethylene glycol (Carbowax 300) and 2 mM sodium cacodylate, pH 7.0. The protein concentration was about 1 mg·mL⁻¹.

Raman Spectroscopy. Raman spectra were measured with a T64000 Raman spectrometer (Jobin-Yvon, France) equipped with an Innova 90–5 argon ion laser (Coherent, U.S.A.). For excitation the 488 nm line was used, the Rayleigh light scattering was removed with a Notch filter, and the Raman scattering was detected with a CCD device. Protein solutions (19 mg·mL⁻¹) were measured at 23 °C in the macro chamber with a 90° setup. Data were analyzed with the software package Spectramax (Jobin-Yvon) supplemented by some of our own programs.

Differential Scanning Calorimetry. DSC measurements were performed as described earlier (Welfle et al., 1992) using the precision scanning microcalorimeter DASM-4 (Institute of Protein Research Pushchino, Russia). In all experiments, the heating rate and the protein concentration were 1 K·min⁻¹ and about 1.50 mg·mL⁻¹, respectively. The

DSC Origin software package (MicroCal Inc., Northampton, MA) was used for data analysis.

ANS Binding. Separate samples for each point were prepared in 2 mM sodium cacodylate, pH 7.0, at various Gdn/HCl concentrations or at different pH values and incubated over night at room temperature. Then the protein samples were mixed with aliquots of an ANS stock solution yielding samples of 1 μ M protein and 20 μ M ANS. These mixtures were incubated for 2 h at 25 °C before the registration of the fluorescence spectra. The concentration of the ANS stock solution in methanol was determined using a molar extinction coefficient of $6.8 \times 10^3 \text{ M}^{-1}\text{cm}^{-1}$ at 370 nm (Mann & Matthews, 1993).

Equilibrium Unfolding and Refolding Studies. Denaturant-dependent conformational transitions were monitored measuring changes of the circular dichroism at 220 nm. Separate samples for each point were made with a protein concentration of 0.080 mg·mL⁻¹. For refolding experiments IF2C was first unfolded by incubation in the presence of 7 M Gdn/HCl for at least 6 h at room temperature and then refolded by addition of renaturation buffer. All solutions were incubated overnight at room temperature and were measured at 25 °C. Concentrations of Gdn/HCl stock solution in the appropriate buffers were determined from refractive index measurements (Pace et al., 1989).

Data Analysis. The fraction of unfolded protein f_u was calculated as recently described (Pace et al. 1989). Assuming one "two-state" or two separate "two-state" transitions of unfolding the free energy changes ΔG_{NI} between native and intermediate state (N \rightarrow I), ΔG_{IU} between intermediate and unfolded state (I \rightarrow U), and ΔG_{AUa} between acid-induced and unfolded state (A \rightarrow U_a) were calculated according to the following equations

$$\Delta G_{\text{NI}} = -RT \ln(F_{\text{N}} - F)/(F - F_{\text{I}}) \quad (1)$$

$$\Delta G_{\text{IU}} = -RT \ln(F_{\text{I}} - F)/(F - F_{\text{U}}) \quad (2)$$

and

$$\Delta G_{\text{AUa}} = -RT \ln(F_{\text{A}} - F)/(F - F_{\text{Ua}}) \quad (3)$$

where F is the observed ellipticity, F_{N} , F_{I} , F_{A} , F_{U} , and F_{Ua} are the ellipticities of the native, intermediate, acid-induced, and unfolded forms at neutral and acidic pH, respectively, R is the gas constant, and T is the absolute temperature. Values for F_{N} , F_{I} , F_{A} , F_{U} , and F_{Ua} in the transition regions were obtained by linear extrapolation from the baseline regions. The stabilities of the native, intermediate, and acid-induced states in the absence of denaturant were determined by a linear least-squares analysis according to the following equations

$$\Delta G_{\text{NI}} = \Delta G_{\text{NI}}^{\text{H}_2\text{O}} - m_{\text{NI}}[\text{denaturant}] \quad (4)$$

$$\Delta G_{\text{IU}} = \Delta G_{\text{IU}}^{\text{H}_2\text{O}} - m_{\text{IU}}[\text{denaturant}] \quad (5)$$

$$\Delta G_{\text{AUa}} = \Delta G_{\text{AUa}}^{\text{H}_2\text{O}} - m_{\text{AUa}}[\text{denaturant}] \quad (6)$$

where ΔG_{NI} , ΔG_{IU} , and ΔG_{AUa} are free energy differences at a given concentration of Gdn/HCl; $\Delta G_{\text{NI}}^{\text{H}_2\text{O}}$, $\Delta G_{\text{IU}}^{\text{H}_2\text{O}}$, and $\Delta G_{\text{AUa}}^{\text{H}_2\text{O}}$ are the free energy differences of the native, intermediate, and acid-induced states extrapolated to 0 M

Gdn/HCl, and m_{NI} , m_{IU} , and m_{AUa} are parameters which describe the cooperativity of the unfolding transition.

The enthalpy difference ΔH_{m} between the folded and unfolded state and the half-transition temperature T_{m} were calculated according to the van't Hoff equation using a nonlinear regression analysis assuming a linear dependence of the ellipticity of the native and unfolded states of IF2C on the temperature.

RESULTS

Aggregation Behavior of IF2C. The IF2C domain was expressed as a fusion protein in *E. coli* and starts with the N-terminal amino acid Ser₅₂₀ (Spurio et al., 1993). It contains 222 amino acids and has a calculated molar mass of 24 452 g·mol⁻¹. The IF2C sample used in this study was 95% pure as estimated by gel electrophoresis.

The elution behavior of IF2C on a Superose 12 column is strongly influenced by the ionic strength of the buffer. In 2 mM sodium cacodylate buffer, pH 7.0, the protein elutes at a position close to V_0 of the column which has an exclusion limit of about 2×10^6 Da. Obviously, at low ionic strength IF2C forms large, but soluble aggregates which do not have any tendency to precipitate. Addition of NaCl, MgCl₂ or Gdn/HCl to the buffer increases the elution volumes of IF2C. This indicates the ionic strength dependent dissociation of the large aggregates and the final formation of monomers. In buffer containing 0.05 M NaCl the elution peak reaches the dimer position, in 0.5 M NaCl molecular weights of about 30–35 kDa with respect to the elution position of globular reference proteins are found indicating the presence of dimers and monomers. Further increase of the ionic strength up to 1.5 M NaCl increases the elution volumes close to the position expected for IF2C monomers.

MgCl₂ dissociates IF2C aggregates more effectively than NaCl and monomers are found already at 0.1 M MgCl₂. Gdn/HCl has depending on its concentration two effects on the elution behavior of IF2C. First, below 0.5 M Gdn/HCl the elution peaks of IF2C shift to higher elution volumes and reach at 0.5 M the presumed monomer/dimer position, reflecting the dissociation of IF2C aggregates. Second, above 0.5 M Gdn/HCl the IF2C elution peaks shift again to lower elution volumes. This is possibly caused by Gdn/HCl binding but not by partial unfolding because peptide CD spectra measured at Gdn/HCl concentrations up to 1.5 M do not provide hints for unfolding.

Secondary Structure and Conformational Changes of IF2C. CD spectra of IF2C were measured in the far-ultraviolet region at various solvent conditions as shown in Figure 1A. The spectra of the native protein (traces 1 and 2) are typical for a mixture of α -helical and β -sheet structures. A spectrum with basically similar characteristics was obtained at pH 2.0 for the acid-induced conformation (A-form) of the protein (trace 3) while the spectrum in the presence of Gdn/HCl is typical for a random-coil structure (trace 4).

The secondary structure content was calculated with the variable selection method (Johnson, 1990). Since we observed strong effects on the aggregation state of IF2C depending on the concentration of sodium or magnesium salts it was of interest to determine the secondary structure of IF2C at the respective buffer conditions. It turned out that the content of secondary structures of IF2C is similar in the aggregated and in the dissociated, low molecular weight form.

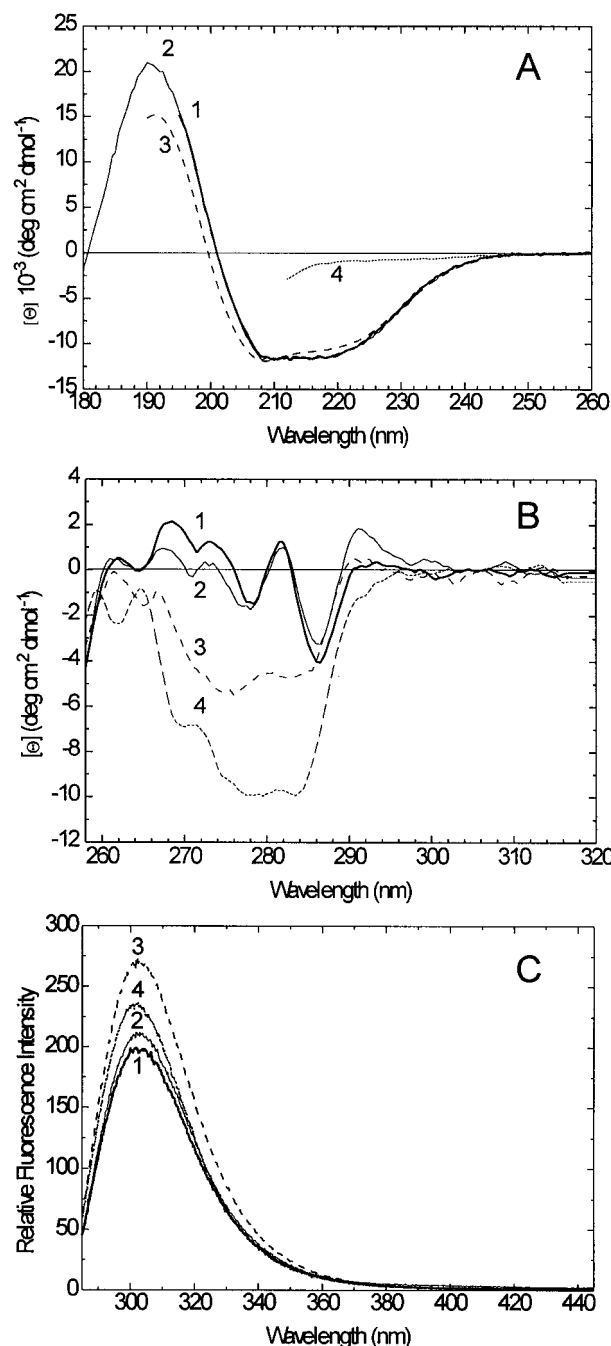


FIGURE 1: Spectroscopic characterization of IF2C. Far-UV CD spectra (A), near-UV CD spectra (B), and fluorescence spectra (C) were recorded in 2 mM sodium cacodylate, pH 7.0, 0.5 M NaCl, 5 mM MgCl_2 (1), in 2 mM sodium cacodylate, pH 7.0 (2), in 10 mM HCl, pH 2.0 (3), and in 2 mM sodium cacodylate, pH 7.0 containing 6.0 M Gdn/HCl (4). Spectrum 4 is truncated at 210 nm because of the strong increase of the absorption of 6 M Gdn/HCl at shorter wavelengths. The spectra were recorded at 25 °C and at protein concentrations of 0.4 $\text{mg}\cdot\text{mL}^{-1}$ (far-UV region), 3.9 $\text{mg}\cdot\text{mL}^{-1}$ (near-UV region), and 0.080 $\text{mg}\cdot\text{mL}^{-1}$ (fluorescence).

23% α -helix, 29% β -sheet, and 19% turn structures were obtained for the aggregated form of IF2C from the spectrum measured in the low ionic strength buffer with 2 mM sodium cacodylate, pH 7.0 (Table 1). Because of the high absorption of 0.5 M NaCl in the far-ultraviolet region the spectrum of IF2C measured in 50 mM sodium phosphate buffer, pH 7.0, 3 mM MgCl_2 was taken for the calculation of the secondary structure content of the dissociated form of IF2C. The secondary structure content is very similar to that found for

Table 1: Secondary Structure Content of IF2C (in %)

helix	β -sheet		turn	remainder
	antiparallel	parallel		
25 (± 1) ^a	23 (± 2)	8 (± 0)	16 (± 1)	29 (± 1)
23 (± 1) ^b	22 (± 1)	7 (± 0)	19 (± 0)	30 (± 1)
26 (± 1) ^c	21 (± 1)	7 (± 1)	19 (± 0)	27 (± 1)
27 ^d	21		19	33

^a Buffer solutions are 50 mM sodium phosphate, 3 mM MgCl_2 , pH 7.0. ^b 2 mM sodium cacodylate, pH 7.0. ^c 20 mM sodium phosphate, pH 2.6. The content of secondary structure was calculated with the program VARSC11 (Johnson, 1990). ^d The result of a secondary structure prediction according to the method of Rost and Sander (1994) is also shown; all amino acid residues with an expected average accuracy > 82% are counted for the calculated % values. Remainder is the difference between the sum of helix, β -sheet and turn, and 100% secondary structure.

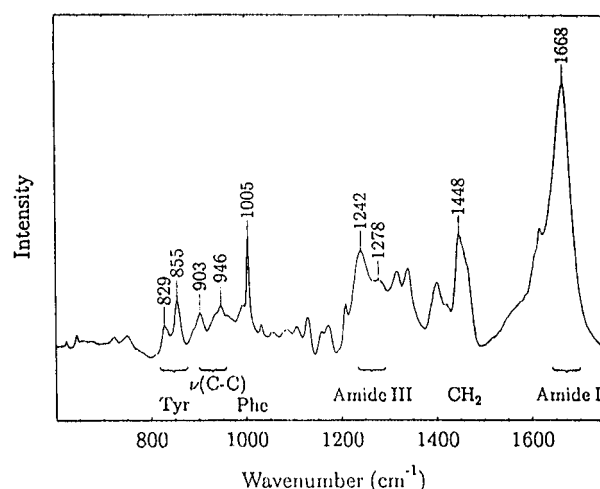


FIGURE 2: Raman spectrum in the region 600–1760 cm^{-1} of IF2C. Labels indicate the frequencies in cm^{-1} , and assignments of major bands are as discussed in the text. Protein concentration 19 $\text{mg}\cdot\text{mL}^{-1}$ in 20 mM HEPES/potassium hydroxide, pH 6.6, 5 mM MgCl_2 .

the aggregated form (Table 1). Variation of ionic strength (up to 1.0 M NaCl) and protein concentration (0.1–1.0 $\text{mg}\cdot\text{mL}^{-1}$) gives rather similar CD spectra. Thus, the aggregation of IF2C to large particles observed at low ionic strength as shown by FPLC is not connected with significant changes in the secondary structure.

Lowering the pH to 2.0, the type of the CD spectrum does not change much but a reduced intensity of the maximum at about 190 nm and a shift of the zero transition indicate small conformational changes. Together with other results, described later, it is evident that IF2C exists in a specific, acid-induced conformation (called A-form) at pH 2–3. In agreement with the qualitative similarity of the spectra comparable values of secondary structure elements were found for the A-form and the native conformation of IF2C (Table 1).

From Raman measurements additional information was obtained on the secondary structure of IF2C (Figure 2). The position of the main peak of the conformation sensitive amide I band centered near 1668 cm^{-1} points to a dominant portion of non- α -helical secondary structures. The amide III band centered near 1242 cm^{-1} also indicates the presence of a significant portion of β -structures. A small spectral component of the amide III band near 1278 cm^{-1} and the C–C stretch band at 946 cm^{-1} are characteristic for α -helix

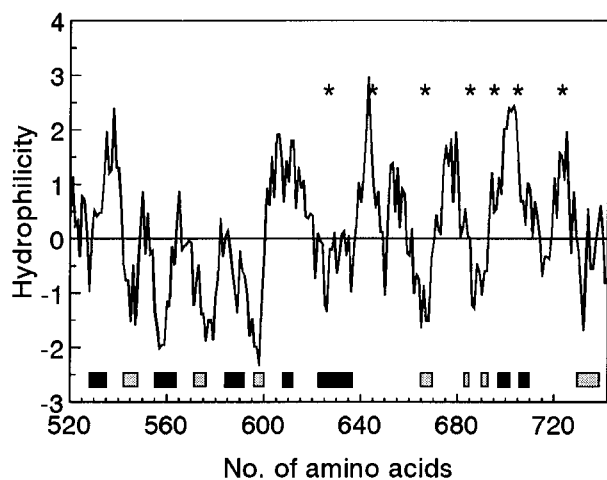


FIGURE 3: Hydrophilicity and secondary structure prediction of IF2C. The hydrophilicity plot was calculated according to Kyte and Doolittle (1982) by using a sliding average of seven amino acid residues. Inset: Secondary structure prediction according to the method of Rost and Sander (1994). α -Helical regions and β -strands are indicated by black and shaded squares, respectively. The positions of the seven tyrosine residues are also shown (stars).

(Peticolas, 1995). Both qualitative conclusions are in accordance with the results of the CD measurements.

Prediction of Secondary Structures. The secondary structures of IF2C were predicted (Figure 3) according to the method of Rost and Sander (1994). The predicted contents is in reasonable agreement with the experimental values and supports the classification of IF2C as an $\alpha + \beta$ protein with a high portion of regularly folded secondary structure elements. The prediction indicates an asymmetric distribution of secondary structure elements with a higher amount in the more hydrophobic N-terminal half of the molecule (Figure 3).

CD and Fluorescence Properties of the Aromatic Amino Acids. IF2C contains no tryptophan residues, four phenylalanine residues, and seven tyrosine residues at positions 625, 643, 669, 691, 701, 712, and 733 (Brombach et al., 1986). CD spectra in the near-ultraviolet region are shown in Figure 1B. The peaks above 270 nm can be attributed to the tyrosine residues of IF2C. The ellipticity of IF2C under native conditions (Figure 1B, traces 1 and 2) is very small, not dependent on the ionic strength, and in a range usually found for unfolded proteins. The spectra indicate a low asymmetry of the electronic configurations of the tyrosine residues which is compatible with a high mobility and surface localization (Strickland, 1974). The fine structure of the CD spectra is reduced and the negative ellipticity is little increased at pH 2.0 (Figure 1B, trace 3) and in the presence of 6 M Gdn/HCl (Figure 1B, trace 4). The broad and featureless spectra in 6 M Gdn/HCl and at pH 2.0 are typical for proteins with a flexible and disordered tertiary structure (Strickland, 1974).

Figure 1C shows the fluorescence spectra of IF2C at high (trace 1) and low (trace 2) ionic strength, of the A-form (trace 3) and of Gdn/HCl-unfolded IF2C (trace 4). The position of the fluorescence maxima at about 305 nm is characteristic for tyrosine emission and independent of the folding state of the protein. Unfolding (Figure 1C, trace 4) or acid-induced conformational change (Figure 1C, trace 3) of IF2C results in an increase of the fluorescence quantum yield. Comparison of the fluorescence spectra of IF2C at high (trace

Table 2: Number of Exposed Tyrosine Residues of IF2C^a

medium	perturbant ^b	λ (nm)	number of exposed residues
buffer	DMSO	286	4.6
buffer	DMSO	279	5.8
buffer	Carbowax 300	286	6.2

^a Buffer is 2 mM sodium cacodylate, pH 7.0. ^b 20% (v/v).

1) and low (trace 2) ionic strength shows that the aggregation state of the protein does not influence significantly the fluorescence quantum yield.

Localization of the Tyrosine Residues of IF2C According to Solvent Perturbation Measurements. The spectra of IF2C and of the model compound *N*-acetyl-L-tyrosine ethyl ester were measured under identical buffer conditions. The effects of the solvents dimethyl sulfoxide [20% (v/v)] and polyethylene glycol [Carbowax 300, 20% (v/v)] on the spectra were determined and used for the calculation of solvent-induced difference spectra. Both dimethyl sulfoxide and polyethylene glycol can be classified tentatively as short-range perturbants with an effective diameter of about 2.0 and 9.2 Å, respectively (Kronman & Robbins, 1970). From the comparison of the protein difference spectra with the difference spectra of the model compound, the number of exposed tyrosine residues can be calculated (Kronman & Robbins, 1970). Similar accessibility values for both perturbants were calculated (Table 2). Thus, about five to six tyrosine residues (70–85%) are localized on the surface of the protein and accessible to both perturbants. This high extent of accessibility is in agreement with the low asymmetry of the environment of tyrosine residues indicated by the low circular dichroism in the aromatic region.

Localization of the Tyrosine Residues of IF2C According to the Raman Spectra. Information about the localization of tyrosine residues in proteins can be derived from their Raman spectra (Figure 2). Characteristic tyrosine Raman bands at 829 and 855 cm^{-1} are sensitive to the hydrogen bonding of the phenolic OH groups (Siamwiza et al., 1975). A high intensity ratio I_{855}/I_{829} of about 2.5 indicates that the hydroxyl groups are acceptors of strong hydrogen bonds from positive donor groups. A low ratio of about 0.3 indicates that the hydroxyl groups are donors of strong hydrogen bonds to negative acceptor groups. Ratios between 0.3 and 2.5 were found when the hydroxyl groups act both as donors and acceptors for moderately strong hydrogen bonds. The determined intensity ratio I_{855}/I_{829} of 1.82 of the tyrosine doublet of IF2C represents an average over the hydrogen bonding states of all tyrosines. The value is consistent with a surface localization of the majority of tyrosine residues that are hydrogen bonded to solvent H_2O molecules. The Raman data support the results of the CD measurements in the aromatic region and the data of the perturbation experiments.

Stability of IF2C against Denaturant-Induced Unfolding. In Figure 4 the normalized transition curves of IF2C are shown calculated from changes of the molar ellipticity $[\Theta]$ at 220 nm between 0 and 7 M Gdn/HCl. The curves reflect the denaturant-induced unfolding and refolding at selected ionic conditions. The unfolding of IF2C (Figure 4, full circles) in 2 mM sodium cacodylate buffer, pH 7.0, 0.5 M NaCl, 5 mM MgCl_2 is completely reversible (Figure 4, open circles). There is a slight decrease of the ellipticity between 0 M and 1.5 M Gdn/HCl followed by a first cooperative

Table 3: Gdn/HCl-Induced Unfolding of IF2C^a

	$\Delta G_{\text{NI}}^{\text{H}_2\text{O}}$	m_{NI}	$c_{\text{m,NI}}$	$\Delta G_{\text{IU}}^{\text{H}_2\text{O}}$	m_{IU}	$c_{\text{m,IU}}$	$\Delta G_{\text{AUa}}^{\text{H}_2\text{O}}$	m_{AUa}	$c_{\text{m,AUa}}$
buffer A	6.2	3.0	2.05	12.9	3.1	4.14	—	—	—
buffer A, refolding	6.3	2.7	2.34	10.8	2.6	4.13	—	—	—
buffer B	—	—	—	—	—	—	11.9	3.6	3.31

^a Buffer A is 2 mM sodium cacodylate, pH 7.0, 0.5 M NaCl, 5 mM MgCl₂, and buffer B is 20 mM potassium phosphate, pH 2.6. Units are as follows: $\Delta G^{\text{H}_2\text{O}}$, kcal·mol⁻¹; m , kcal·mol⁻¹·M⁻¹. c_{m} represents the Gdn/HCl transition midpoint concentration. Equilibrium data were fitted assuming “two-state” transitions from the native to the intermediate state and from the intermediate to the unfolded state.

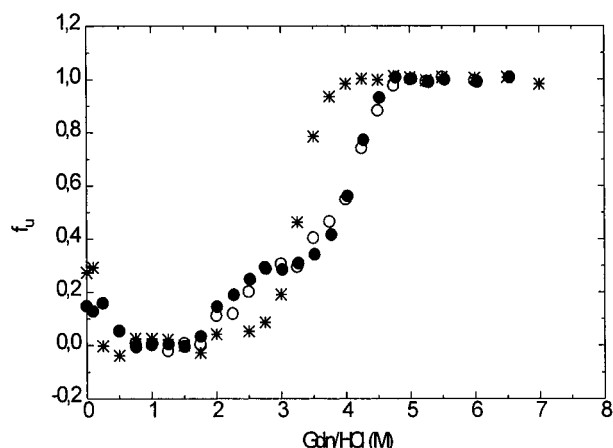


FIGURE 4: Gdn/HCl-induced transitions of IF2C. The normalized unfolding curves (full circles and stars) and refolding curve (open circles) show the fraction of unfolded protein f_u versus the denaturant concentration. The experimental curves were obtained monitoring changes of the ellipticity at 220 nm in 2 mM sodium cacodylate buffer, pH 7.0, 0.5 M NaCl, 5 mM MgCl₂ (circles), and in 20 mM sodium phosphate, pH 2.6 (stars). The measurements were performed at a protein concentration of 0.080 mg·mL⁻¹ at 25 °C.

transition at about $c_{\text{m}} = 2.0$ M Gdn/HCl. About 30% of the total ellipticity change are connected with the first transition. A second cooperative transition is observed between 3.8 and 4.5 M Gdn/HCl with a c_{m} value of about 4.0 M Gdn/HCl.

Assuming two “two-state” transitions, the changes of the free energy $\Delta G^{\text{H}_2\text{O}}$, the slopes m of the plots, and the half-transition concentrations c_{m} of Gdn/HCl were calculated as described in Materials and Methods. The results are summarized in Table 3. The free energy of unfolding $\Delta G_{\text{NI}}^{\text{H}_2\text{O}}$ for the first transition amounts to about 6 kcal·mol⁻¹. For the second transition a $\Delta G_{\text{IU}}^{\text{H}_2\text{O}}$ value of about 13 kcal·mol⁻¹ was obtained. According to these data, IF2C is composed of two subdomains of unequal stability. The total free energy of unfolding between the native (N) and unfolded (U) states of IF2C is about 19 kcal·mol⁻¹. Other small naturally occurring globular proteins have conformational stabilities between 5 and 15 kcal·mol⁻¹ (Pace, 1990). Thus, the sum of the stabilities of the two subdomains is on the upper limit of these values.

For a further characterization of the native, intermediate, and unfolded states, we investigated the binding of ANS to IF2C at increasing concentrations of Gdn/HCl. ANS was used to probe hydrophobic sites in proteins and conformational changes that are accompanied by an exposure of hydrophobic regions (Goto & Fink, 1989; Semisotnov et al., 1991; Horowitz et al., 1995). We could not find any binding of ANS (data not shown) over the whole range of the transition curve. Obviously there is no preferential ANS interaction with the intermediate state. Provided that binding of ANS to hydrophobic clusters is not inhibited at moderate

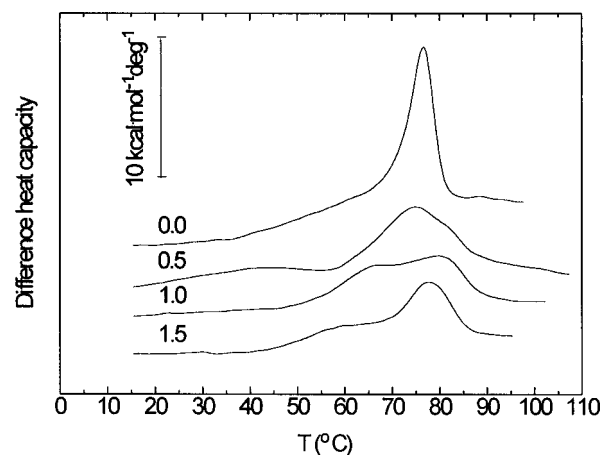


FIGURE 5: Experimental difference heat capacity curves of IF2C. The measurements were performed in 2 mM sodium cacodylate, pH 7.0, containing 0, 0.5, 1.0, or 1.5 M Gdn/HCl.

concentrations of about 2.0 M Gdn/HCl, this result points against a molten globule-like state of the intermediate and is in accordance with the stepwise unfolding of two individual domains.

Temperature-Induced Unfolding of IF2C. Melting experiments in low ionic strength buffer at pH 7.0 are impaired by the appearance of aggregates which precipitate at higher temperatures. We screened for suitable conditions measuring the absorbance at 400 nm where light scattering indicates the formation of aggregates. Temperature induced aggregation is very low in 2 mM sodium cacodylate buffer, pH 7.0, containing 0.5, 1.0, or 1.5 M Gdn/HCl. CD measurements in the peptide region showed that the secondary structure of IF2C is not changed up to 1.5 M Gdn/HCl.

Thermal unfolding of IF2C measured by differential scanning calorimetry was studied in 2 mM sodium cacodylate buffer, pH 7.0, and in the same buffer containing additionally 0.5, 1.0, or 1.5 M Gdn/HCl. In Figure 5 the respective difference heat capacity curves are shown. The reversibility of thermal unfolding was tested in a second scan after cooling down the sample. Only in Gdn/HCl-containing buffers was unfolding partially reversible (not shown).

In Gdn/HCl-free buffer of low ionic strength a sharp peak with a T_{m} value of 76 °C was observed after some premelting effects. With increasing Gdn/HCl concentrations melting shows more complicated biphasic characteristics. The results of deconvolution of the biphasic excess heat capacity functions of IF2C in buffer containing 1.0 or 1.5 M Gdn/HCl are shown in Figure 6 and are summarized in Table 4. At these buffer conditions IF2C is composed of two energetic folding units.

Separate melting of two folding units could not be demonstrated in low ionic strength buffer and in buffer containing 0.5 M Gdn/HCl. Premelting effects at lower temperatures as well as formation of aggregates at higher

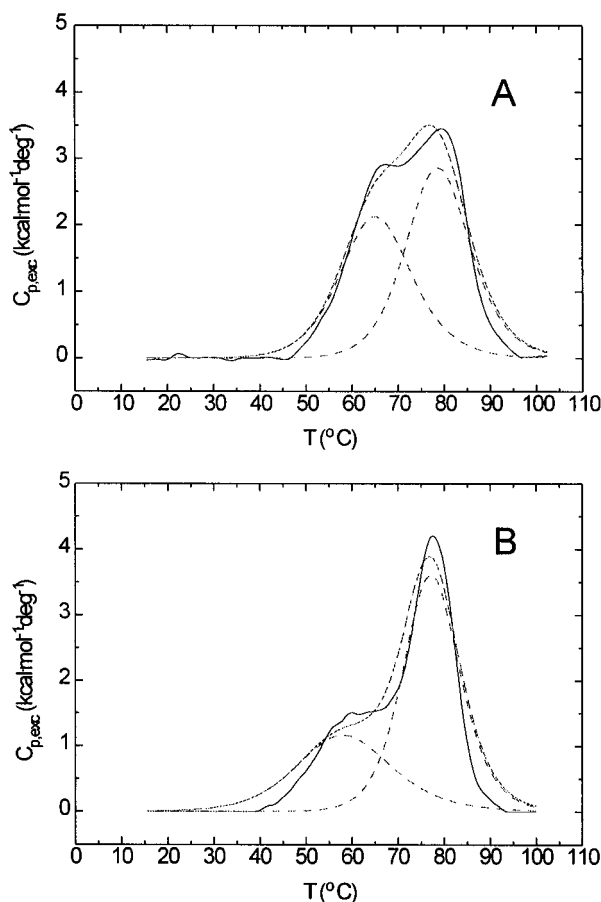


FIGURE 6: Deconvoluted heat capacity function of IF2C. Buffer solution is 2 mM sodium cacodylate, pH 7.0, in the presence of 1.0 M Gdn/HCl (A) and 1.5 M Gdn/HCl (B).

Table 4: Transition Temperatures (T_m) and Enthalpy Changes (ΔH_m) of IF2C

Gdn/HCl (M) ^a	T_m	T_m^1	ΔH_m^1	T_m^2	ΔH_m^2
0	76.0	—	—	—	—
0.5	75.0	—	—	—	—
1.0	—	65.3	42	78.4	56
1.5	—	58.6	32	77.4	60

^a Buffer solution is 2 mM sodium cacodylate, pH 7.0. Units are as follows: T_m , °C; ΔH_m , kcal·mol⁻¹.

temperatures are indicated in the melting curves. Therefore, the deconvolution of these excess heat capacity functions is not justified.

Characterization of the Acid-Induced Conformation (A-Form) of IF2C. Very similar CD spectra of IF2C are found in the pH range from 11.0 to 3.0. Lowering the pH from 3.0 to 2.0 leads to a small decrease of the ellipticities at 220 nm and 195 nm and a small blue shift of the zero transition point in comparison to IF2C at pH 7.0 (Figure 1A, trace 3). The features of the CD spectrum obtained at pH 1.0 are characteristic of the induction of additional β -structures. Upon raising the pH again to neutral pH, the observed spectral changes are completely reversible.

ANS binding studies were performed to characterize the hydrophobicity of the protein surface and were used to study protein folding intermediates such as the molten globule state (Goto & Fink, 1989; Semisotnov et al., 1991; Misselwitz et al., 1995). The binding of ANS to hydrophobic clusters of a protein is connected with changes in the ANS fluorescence features, namely an increase of the fluorescence intensity

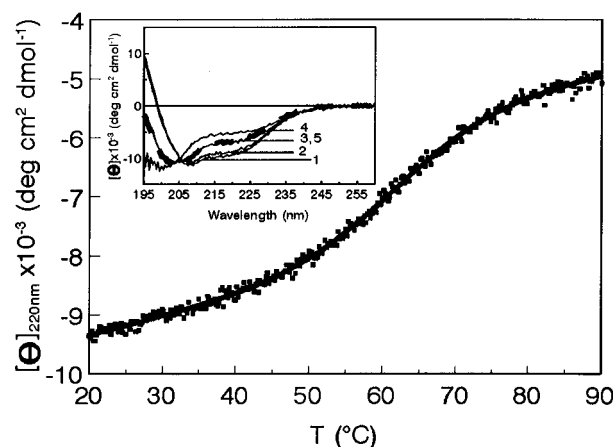


FIGURE 7: Temperature-induced unfolding of IF2C at pH 2.0. The temperature-induced unfolding was monitored by changes of the ellipticity at 220 nm in 5 mM sodium phosphate, pH 2.0. The heating rate was 20 °C·h⁻¹, and the protein concentration 0.1 mg·mL⁻¹. The squares are the experimental data points and the solid line represents the fitted data taking a linear dependence of the ellipticities in the pre- and post-melting range. The calculated transition temperature T_m and the molar enthalpy change ΔH_m are 67.1 °C and 29.6 kcal·mol⁻¹, respectively. Inset: Far-UV spectra of IF2C at 10 °C (1), 30 °C (2), 60 °C (3), and 90 °C (4) and of the refolded form at 10 °C (5).

and a blue shift of the fluorescence emission maximum from about 520 nm to 470 nm (Stryer, 1965; Turner & Brand, 1968). ANS fluorescence spectra in the presence of IF2C were measured at various pH values between 1.0 and 6.0 (data not shown). At pH 6.0, 4.0, and 1.0 a very small increase and blue shift of the ANS fluorescence was observed in the presence of protein in comparison to free ANS. But, an about eight times higher ANS fluorescence intensity and a shift of the fluorescence maximum to about 475 nm is indicated at pH 3.0 and 2.0. The data demonstrate the ability of the A-form to bind ANS.

In an attempt to determine the stability of the A-form, changes of the mean molar ellipticity $[\Theta]$ at 220 nm were monitored depending on increasing temperatures or Gdn/HCl concentrations. The thermal unfolding curve at low ionic strength (5 mM sodium phosphate, pH 2.0) is shown in Figure 7. The appearance of an isodichroic point at about 205 nm (inset of Figure 7) suggests that only folded and unfolded IF2C molecules are present at equilibrium. The cooperativity of the transition is low. The half transition temperature T_m of 67 °C is about 10 °C lower than the T_m value in low ionic strength buffer at pH 7.0, determined microcalorimetrically (see Figure 5, upper curve). Assuming a “two-state” transition for the unfolding of the A-form a ΔH_m value of 29.6 kcal·mol⁻¹ was calculated from the unfolding curve in Figure 7.

Gdn/HCl-induced unfolding of the A-form at pH 2.6 proceeds with high cooperativity. Unfolding starts at a Gdn/HCl concentration of about 2.8 M and reaches plateau values at about 4.5 M (Figure 4, stars). Assuming a “two-state” mechanism of unfolding, we calculated a free energy of unfolding $\Delta G_{A_{Ua}}^{H_2O}$ of about 12 kcal·mol⁻¹ (Table 3). The sigmoidal transition curve and the relatively high $\Delta G_{A_{Ua}}^{H_2O}$ value are compatible with a rather compact, folded conformation of the A-form. The stability of the A-form is surprisingly high in comparison to the stability of acid-induced forms of other proteins [e.g., 1.3 kcal·mol⁻¹ for α -lactalbumin (Ikeguchi et al., 1992), 2.1 kcal·mol⁻¹ for

apomyoglobin (Barrick & Baldwin, 1993), and $3.0 \text{ kcal}\cdot\text{mol}^{-1}$ for HIV-1 rp24 (Misselwitz et al., 1995)].

At low concentrations of Gdn/HCl additional secondary structures are induced in IF2C prior to its unfolding at higher denaturant concentrations. This is indicated by the increasing negative ellipticity at 220 nm which we observed in the Gdn/HCl concentration range 0–0.5 M (Figure 4). Similar results were recently described for other proteins under acidic conditions (Hagihara et al., 1994; Misselwitz et al., 1995) and are discussed as an effect of Gdn/HCl interactions with charged groups of the protein.

Proteolytic degradation of IF2C by pepsin at pH 2.6 (data not shown) points to the preservation of a folded and relatively resistant core region under acidic condition. Two relatively stable fragments with molar masses of about 15 000 and 5 000 $\text{g}\cdot\text{mol}^{-1}$ were obtained.

DISCUSSION

The C-domain of the translational initiation factor IF2 from *B. stearothermophilus* is relatively resistant to degradation by various proteolytic enzymes (Severini et al., 1990; Gualerzi et al., 1991). In agreement with these results, the physicochemical data presented in this study characterize IF2C as a protein with a folded structure of rather high thermodynamic stability. Extending earlier observations, the data clearly demonstrate that IF2C consists of two subdomains.

The two-domain composition of IF2C is most evident from the biphasic denaturant-dependent unfolding and refolding curves of IF2C at neutral pH. Unfolding of IF2C proceeds in two transition steps and involves at least one significantly populated intermediate state (I-form). The two transitions from the native state to the I-form and from the I-form to the unfolded state are well separated. Both transitions can be described by a "two-state" mechanism. Therefore, the observed two-step unfolding probably reflects an independent consecutive unfolding of subdomains 1 and 2. The first transition is characterized by a decrease in the α -helix content of about 30%. Secondary structure prediction according to Rost and Sander (1994) shows that about 20% of the total α -helices are localized in the C-terminal part of IF2C (Figure 3). This value is in reasonable agreement with the reduction of the α -helix content during the first transition and suggests a C-terminal localization of the corresponding subdomain 1. The prediction indicates an asymmetric distribution of secondary structure elements, with a higher amount in the more hydrophobic N-terminal half and a lower amount in the more hydrophilic C-terminal part of IF2C. Remarkably, the C-terminal portion of the molecule contains a cluster of six out of a total of seven tyrosine residues (Figure 3). Nevertheless, it is not possible to obtain further support for the tentative assignment of the subdomains from aromatic CD and fluorescence measurements. Most of the tyrosine residues are surface localized in the folded state, and, therefore, a significant spectral effect cannot be expected during unfolding of this region.

The results of ANS binding argue against a molten globule-like structure of the I-form of IF2C. Rather, they are compatible with an intermediate state where subdomain 1 is already unfolded while subdomain 2 is still folded. Also microcalorimetric measurements clearly show the melting of two separate subdomains. Therefore, the unfolding of

IF2C can be reasonably described by an independent domain unfolding model.

Taken together, the secondary structure and the hydrophilicity predictions as well as the distribution of the tyrosines and the bimodal unfolding behavior of the molecule demonstrate that the IF2 C-domain consists of two subdomains with different structural properties and stability. It is noteworthy, in this context, that all the mutations affecting the interaction of IF2C with initiator-tRNA which have been identified so far seem to be localized in the C-terminal subdomain, while several mutations introduced in the N-terminal subdomain did not result in a detectable phenotype (R. Spurio, E. Caserta, L. Brandi, and C. O. Gualerzi, unpublished observations). Thus, it would appear that the two subdomains are not only structurally but also functionally distinct.

IF2C molecules have a strong tendency to form soluble aggregates at low ionic strength. At 1.5 M NaCl or in the presence of 0.1 M MgCl_2 , however, they exist mainly as monomers. The aggregation state of IF2C has no pronounced influence on the conformation of the protein as shown by CD measurements at various ionic strengths and protein concentrations. Furthermore, the accessibility of tyrosine residues to perturbant molecules is not influenced by the aggregation state. Thus, monomers must associate in such way that their surfaces remain accessible to solvent molecules. This may be accomplished by the formation of loose, solvent penetrable aggregates. Another possibility might be the formation of extended structures with small contact sites. In this case, only small parts of the monomer surfaces would be covered but most of the surfaces would remain solvent accessible. At present, the structure of the aggregates and likewise the potential functional significance of the association behavior remain open questions. It should be recalled in this connection, however, that none of the functional properties of IF2 or of its known mechanism of action requires the participation of a molecule having anything other than a monomeric structure.

Acid-induced conformational changes have been described for a variety of proteins (Fink et al., 1994). The A-form of IF2C is characterized by the following features: first, a secondary structure content comparable to that at neutral pH; second, a reduced fine structure of the aromatic CD; and third, a strong binding of ANS. The A-form resembles in some features the molten globule state that is characterized as a compact denatured state with a significant native-like secondary structure and a fluctuating tertiary structure (Ptitsyn, 1995). The spectral features of IF2C at low pH are typical of type II proteins according to the classification of acid denaturation of proteins (Fink et al., 1994). Such proteins (e.g., α -lactalbumin and carbonic anhydrase) turn from the native state directly into a molten globule-like A state and do not pass through an unfolded intermediate state.

The Gdn/HCl-induced unfolding of the A-form differs markedly from IF2C unfolding at neutral pH. Only one cooperative transition with a free energy of unfolding $\Delta G_{\text{A} \rightarrow \text{U}}^{\text{H}_2\text{O}}$ of $11.9 \text{ kcal}\cdot\text{mol}^{-1}$ is observed at low pH instead of two transitions at neutral pH. The stability of the A-form is similar to that of subdomain 2 at neutral pH. However, this does not indicate that the structure of the A-form is similar to that discussed for the I-form with unfolded subdomain 1 and folded subdomain 2. Spectroscopic differences between A- and I-form and differences in ANS

binding argue against this possibility. It is more probable that the structure of the A-form is composed of residues of both subdomains of IF2C which have changed conformation and stability at low pH.

The physicochemical properties of IF2C described in this work enlighten a relatively small part of IF2. Nevertheless, the identification of two subdomains of IF2C having distinct physicochemical, structural and possibly functional properties should prove particularly valuable for the overall structural characterization of this domain of IF2, in combination with the X-ray crystallography and multinuclear NMR spectroscopic studies which are presently in progress. Finally, in combination with the genetic studies aimed at identifying the functionally relevant amino acid residues, we can expect a complete understanding of the structure and structural-functional basis for the recognition and interaction of IF2 with the initiator tRNA.

ACKNOWLEDGMENT

We thank Mrs. B. Kannen for skillful technical assistance and Dr. O. Ristau for his help in the use of computer programs.

REFERENCES

- Barrick, D., & Baldwin, R. L. (1993) *Biochemistry* 32, 3790–3796.
- Brombach, M., Gualerzi, C. O., Nakamura, Y., & Pon, C. L. (1986) *Mol. Gen. Genet.* 205, 97–102.
- Cenatiempo, Y., Deville, F., Dondon, J., Grunberg-Manago, M., Sacerdot, C., Hershey, J. W. B., Hansen, H. F., Petersen, H. U., Clark, B. F. C., Kjeldgaard, M., la Cour, T. F. M., Mortensen, K. K., & Nyborg, J. (1987) *Biochemistry* 26, 5070–5076.
- Clark, B. F. C., Kjeldgaard, M., la Cour, T. F. M., Thirup, S., & Nyborg, J. (1990) *Biochim. Biophys. Acta* 1050, 203–208.
- Fink, A. L., Calciano, L. J., Goto, Y., Kurotsu, T., & Palleros, D. R. (1994) *Biochemistry* 33, 12504–12511.
- Goto, Y., & Fink, L. A. (1989) *Biochemistry* 28, 945–952.
- Gualerzi, C. O., Severini, M., Spurio, R., La Teana, A., & Pon, C. L. (1991) *J. Biol. Chem.* 266, 16356–16362.
- Hagihara, Y., Tan, Y., & Goto, Y. (1994) *J. Mol. Biol.* 237, 336–348.
- Horowitz, P. M., Hua, S., & Gibbons, D. L. (1995) *J. Biol. Chem.* 270, 1535–1542.
- Ikeguchi, M., Sugai, S., Fujino, M., Sugawara, T., & Kuwajima, K. (1992) *Biochemistry* 31, 12695–12700.
- Johnson, W. C., Jr. (1990) *Proteins: Struct., Funct., Genet.* 7, 205–214.
- Kronman, M. J., & Robbins, F. M. (1970) in *Fine structure of proteins and nucleic acids* (Fasman, G. D., Ed.) pp 271–416, Marcel Dekker, New York.
- Kyte, J., & Doolittle, R. K. (1982) *J. Mol. Biol.* 157, 105–132.
- Mach, H., Middaugh, C. R., & Lewis, R. V. (1992) *Anal. Biochem.* 200, 74–80.
- Mann, C. J., & Matthews, C. R. (1993) *Biochemistry* 32, 5282–5290.
- Misselwitz, R., Zirwer, D., Frohne, M., & Hanson, H. (1975) *FEBS Lett.* 55, 233–236.
- Misselwitz, R., Hausdorf, G., Welfle, K., Höhne, W. E., & Welfle, H. (1995) *Biochim. Biophys. Acta* 1250, 9–18.
- Pace, C. N. (1990) *Trends Biochem. Sci.* 15, 14–17.
- Pace, C. N., Shirley, B. A., & Thomson, J. A. (1989) in *Protein structure: A practical approach* (Creighton, T. E., Ed.) pp 311–330, IRL Press, Oxford.
- Pai, E. F., Kregel, U., Petsko, G. A., Goody, R. S., Kabsch, W., & Wittinghofer, A. (1990) *EMBO J.* 9, 2351–2359.
- Pawlik, R. T., Littlechild, J., Pon, C. L., & Gualerzi, C. O. (1981) *Biochem. Int.* 2, 421–428.
- Peticolas, W. L. (1995) *Methods Enzymol.* 246, 389–416.
- Ptitsyn, O. B. (1995) *Adv. Protein Chem.* 47, 83–229.
- Rost, B., & Sander, C. (1994) *Proteins: Struct., Funct., Genet.* 19, 55–72.
- Semisotnov, G. V., Rodionova, N. A., Razgulyaev, O. I., Uversky, V. N., Gripas, A. F., & Gilmanshin, R. I. (1991) *Biopolymers* 31, 119–128.
- Severini, M., Choli, T., La Teana, A., & Gualerzi, C. O. (1990) *FEBS Lett.* 276, 14–16.
- Severini, M., Choli, T., La Teana, A., & Gualerzi, C. O. (1992) *FEBS Lett.* 297, 226–228.
- Shiba, K., Ito, K., Nakamura, Y., Dondon, J., & Grunberg-Manago, M. (1986) *EMBO J.* 5, 3001–3006.
- Siamwiza, M. N., Lord, R. C., Chen, M. C., Takamatsu, T., Harada, I., Matsuura, H., & Shimanouchi, T. (1975) *Biochemistry* 14, 4870–4876.
- Spurio, R., Severini, M., La Teana, A., Canonaco, M. A., Pawlik, R. T., Gualerzi, C. O., & Pon, C. L. (1993) in *The translational apparatus: Structure, function, regulation, evolution* (Nierhaus, K. H., Ed.) pp 241–252, Plenum Press, New York.
- Strickland, E. H. (1974) *Crit. Rev. Biochem.* 2, 113–175.
- Stryer, L. (1965) *J. Mol. Biol.* 13, 482–495.
- Travers, A. A., Debenham, P. E., & Pongs, O. (1980) *Biochemistry* 19, 1651–1656.
- Turner, D. C., & Brand, L. (1968) *Biochemistry* 7, 3381–3390.
- Welfle, H., Misselwitz, R., Welfle, K., Groch, N., & Heinemann, U. (1992) *Eur. J. Biochem.* 204, 1049–1055.

BI962613N